Oligodeoxynucleotides Having a Loop Consisting of 3′-Deoxy-4′-*C*-(2-hydroxyethyl)thymidines Form Stable Hairpins†

Yuji Yamamoto,‡ Satoshi Shuto,*,‡ Yutaka Tamura,§ Tetsuya Kodama,‡ Shuichi Hoshika,‡ Satoshi Ichikawa,‡ Yoshihito Ueno,|| Eiko Ohtsuka,§ Yasuo Komatsu,§ and Akira Matsuda‡

Graduate School of Pharmaceutical Sciences, Hokkaido University, Kita-12, Nishi-6, Kita-ku, Sapporo 060-0812, Japan, National Institute of Advanced Industrial Science and Technology, 2-17-2-1 Tsukisamu-higashi, Toyohira-ku, Sapporo 062-8517, Japan, and Faculty of Engineering, Gifu University, Yanagido, Gifu 501-1193, Japan

Received February 19, 2004; Revised Manuscript Received May 6, 2004

ABSTRACT: Components that form stable hairpin loops are highly useful for the development of functional DNA and RNA molecules. We have designed and synthesized a sugar-modified thymidine analogue, 3′-deoxy-4′-*C*-(2-hydroxyethyl)thymidine (**X**), as a nucleosidic loop component stabilizing the hairpin structure. The ODNs **I-1**−**4**, 5′-d[CGAACG-$\mathbf{X}_n$-CGTTCG]-3′ (**I-1**, $n = 1$; **I-2**, $n = 2$; **I-3**, $n = 3$; **I-4**, $n = 4$), forming the hairpin loop structures, of which the loop moiety consisted of the analogue **X**, and also the corresponding unmodified ODNs **II-1**−**4**, 5′-d[CGAACG-$\mathbf{T}_n$-CGTTCG]-3′ (**II-1**, $n = 1$; **II-2**, $n = 2$; **II-3**, $n = 3$; **II-4**, $n = 4$), having a thymidine loop, were synthesized by the phosphoramidite method. The melting temperatures (T_m) of the ODNs **I-1**−**4** containing **X** in the loop moiety at 5 μM were 67.1, 68.1, 73.0, and 69.3 °C, respectively, and those of the control natural ODNs **II-1**−**4** were 65.3, 67.0, 69.2, and 68.8 °C, respectively. Thus, the ODNs **I-1**−**4** formed a more thermally stable hairpin than the corresponding unmodified ODNs **II-1**−**4** having an equal number of loop residues. The hairpin structures of the modified ODNs **I-1**−**4** and the unmodified ODNs **II-1**−**4** were investigated by CD spectroscopy and molecular mechanics calculations. These results showed that the 4′-branched nucleoside **X** can stabilize hairpin structures when it is present in the loop moiety, probably due to the flexibility of the one-carbon-elongated 4′-branched structure.

Hairpin loops are the dominant secondary structure in RNA and have various functional and structural roles (*1*). In DNA, a number of sequences also have been known to form stable hairpin structures, which could be important in various biological processes, such as DNA replication and transcription (*1*, *2*). DNA hairpin loops are also important as drug targeting sites; for example, in antigene therapy, drug molecules recognize loop structures in a different way from the usual Watson−Crick base-paired double-stranded structures (*3*).

In recent years, there has been growing interest in the development of DNA and its synthetically altered analogues as tools in biological studies and as therapeutic agents. Compared with their corresponding RNA congeners, DNA and its analogues are chemically and biologically stable and also more easily synthesized, which is crucial for their use as biological tools and therapeutics (*4*, *5*). In DNA and its analogues, the hairpin loop structures are important in exerting biological effects. For example, it has been reported that loop structures are essential for the catalytic activity of deoxyribozymes (*4*, *5*), that the hairpin tagging to terminals of functional oligodeoxynucleotides (ODNs)[1] stabilizes them to nucleases (*6*−*8*), and that formation of dumbbell-type ODNs by adding two loops on a double-stranded ODN improves their potency as decoy molecules (*9*, *10*).

Therefore, to develop novel DNA analogues with biological potency, components for the loop moiety, which form thermally stable and nuclease-resistant hairpins, would be extremely useful. Nonnucleotidic synthetic loops have been investigated and, in some cases, make more stable hairpin structures than those possessing natural nucleotidic loops (*11*, *12*). However, the nucleobases in the loops of hairpins are often essential for stabilizing the structure and for exhibiting biological functions, i.e., nucleobases stabilize DNA hairpin loops by hydrogen bonding (*13*−*15*), constitute catalytic sites of deoxyribozymes (*4*, *5*), or interact with DNA-binding proteins (*16*, *17*). From this viewpoint, nucleoside analogues bearing a natural nucleobase, which can form stable hairpin loop structures, would be of great interest.

† This investigation was supported by a Grant-in-Aid for Creative Scientific Research (13NP0401) from the Japan Society for the Promotion of Science. This report constitutes part 227 of Nucleosides and Nucleotides. Part 226: Hoshika, S., Ueno, Y., Kamiya, H., Matsuda, A. (2004)Alternate-strand triple-helix formation by 3′-3′-linked oligodeoxynucleotides composed of asymmetrical sequences, *Bioorg. Med. Chem. Lett.* (in press).

* Corresponding author: phone +81-11-706-3229; fax +81-11-706-4980; e-mail shu@pharm.hokudai.ac.jp.

‡ Hokkaido University.

§ National Institute of Advanced Industrial Science and Technology.

|| Gifu University.

[1] Abbreviations: ODN, oligodeoxynucleotide; MALDI-TOF MS, matrix-assisted laser desorption/ionization time-of-flight mass spectrometry; OPLS-AA, optimized potentials for liquid simulations, all atom; GB/SA, generalized Born/surface area; TBSCl, *tert*-butyldimethylsilyl chloride; DMF, *N*,*N*-dimethylformamide; THF, tetrahydrofuran; FAB, fast atom bombardment; HRMS, high-resolution mass spectrometry; DMTr, dimethoxytrityl; HPLC, high-performance liquid chromatography.

10.1021/bi0496283 CCC: $27.50
Published on Web 06/18/2004

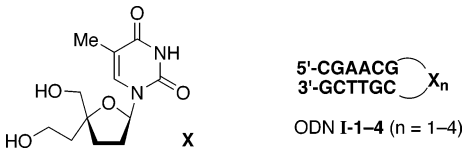

FIGURE 1: 4′-Branched thymidine analogue **X** and hexameric stem hairpin sequences of ODNs **I-1**−**4**.

With these findings and considerations in mind, we designed and synthesized a sugar-modified thymidine analogue, 3′-deoxy-4′-*C*-(2-hydroxyethyl)thymidine (**X**, Figure 1), as a component of loops, that is able to stabilize the hairpin structure. The ODNs **I-1**−**4** (Figure 1), 5′-d[C-GAACG-$\mathbf{X}_n$-CGTTCG]-3′ (**I-1**, $n = 1$; **I-2**, $n = 2$; **I-3**, $n = 3$; **I-4**, $n = 4$), forming the hairpin loop structures, of which the loop moiety consisted of the analogue **X**, were synthesized. The thermal stability, susceptibility to a nuclease, and structures of these ODNs were investigated. This report describes the detailed results of these studies.

EXPERIMENTAL PROCEDURES

General Methods. NMR data are reported in parts per million (ppm) downfield from Me_4Si (^1H) or H_3PO_4 (^{31}P). Silica gel chromatography was performed with Merck silica gel 5715 or 9385 (neutral). Reactions were carried out under an argon atmosphere.

3′-O-(tert-Butyldimethylsilyl)thymidine (**6**). A mixture of thymidine (10.3 g, 40 mmol), imidazole (11.4 g, 168 mmol), and TBSCl (12.6 g, 84 mmol) in DMF (150 mL) was stirred at room temperature for 15 h, and then EtOH (50 mL) was added. The resulting mixture was partitioned between AcOEt and H_2O, and the organic layer was washed with aqueous saturated $NaHCO_3$, H_2O, and brine, dried, and evaporated. A solution of the residue in THF/H_2O/trifluoroacetic acid (TFA) (4:1:1, 600 mL) was stirred at 0 °C for 2 h and then aqueous saturated Na_2CO_3 (600 mL) was added. The resulting mixture was extracted by AcOEt (5 times), and the extract was washed with brine, dried (Na_2SO_4), and evaporated. The residue was purified by column chromatography (silica gel; AcOEt/hexane 1:3−1:1) to give **6** (8.4 g, 59%) as a foam: ^1H NMR ($CDCl_3$, 270 MHz) δ 8.43 (br s, 1 H, NH-3), 7.63 (d, 1 H, H-6, $J = 1.3$ Hz), 6.13 (dd, 1 H, $J = 6.8, 6.8$ Hz), 4.50 (m, 1 H, H-3′), 3.92 (dd, 1 H, H-5′a, $J = 2.5, 12.4$ Hz), 3.75 (dd, 1 H, H-5′b, $J = 3.5, 12.4$ Hz), 2.35 (m, 1 H, H-2′a), 2.21 (ddd, 1 H, H-2′b, $J = 3.9, 6.8, 13.3$ Hz), 1.92 (s, 3 H, CH_3-5), 0.90 [s, 9 H, Si-C(CH_3)$_3$], 0.09 (s, 6 H, 2Si-CH_3); MS (FAB) *m/z* 357 (MH^+).

4′-Phenylselenothymine Derivative (**5**). A mixture of **6** (14.7 g, 41.2 mmol) and Dess−Martin periodinate (*18*) (18.4 g, 43.3 mmol) in CH_2Cl_2 (400 mL) was stirred at room temperature for 1 h, and then aqueous saturated $Na_2S_2O_3$ (80 mL) and aqueous saturated $NaHCO_3$ (320 mL) were added. The organic layer was separated and evaporated to give crude **7** as the residue. To a solution of the residue in CH_2Cl_2 (200 mL) was added slowly a cooled (−78 °C) solution of PhSeCl (23.7 g, 124 mmol) and Et_3N (34.4 mL, 247 mmol) in CH_2Cl_2 (210 mL) at −78 °C, and then the mixture was stirred at 4 °C for 20 h (*19*). After addition of AcOEt (100 mL) and H_2O (100 mL), the resulting mixture was partitioned, and the organic layer was washed with brine, dried (Na_2SO_4), and evaporated. The residue was purified by column chromatography (silica gel; AcOEt/hexane, 1:1−3:1) to give **5** (17.5 g, 83%) as a foam: ^1H NMR ($CDCl_3$, 270 MHz) δ 9.76 (s, 1 H, CHO), 8.51 (br s, 1 H, NH-3), 7.57 (d, 1 H, H-6, $J = 1.1$ Hz), 6.32 (dd, 1 H, H-1′, $J = 5.8, 8.1$ Hz), 4.67 (m. 1 H, H-3′), 4.16 (m, 1 H, H-4′), 2.32 (m, 1 H, H-2′a, $J = 2.4, 5.8, 13.4$ Hz), 2.05 (m, 1 H, H-2′b), 1.96 (s, 3 H, CH_3-5), 0.92 [s, 9 H, Si-C(CH_3)$_3$], 0.14 (s, 3 H, Si-CH_3), 0.09 (s, 3 H, Si-CH_3); MS (FAB) *m/z* 510 (MH^+).

5′-O-Dimethoxytrityl-4′-C-(2-((tert-butyldimethylsilyl)oxy)-ethyl)thymidine (**8**). A mixture of **3** (9.0 g, 15 mmol), which was prepared from **5** according to the previous method (*20*), 2,6-lutidine (4.0 mL, 34 mmol), and TBSOTf (4.8 mL, 21 mmol) in CH_2Cl_2 (51 mL) was stirred at −40 °C for 3 h, and then aqueous saturated $NaHCO_3$ was added. The resulting mixture was partitioned between AcOEt and H_2O, and the organic layer was washed with brine, dried (Na_2SO_4), and evaporated. The residue was purified by column chromatography (silica gel; AcOEt/hexane, 2:3−1:0) to give **8** (9.0 g, 88%) as a foam: ^1H NMR ($CDCl_3$, 400 MHz) δ 8.03 (s, 1 H, NH-3), 7.71 (s, 1 H, H-6), 7.14 (m, 13 H, Ar-H), 6.48 (dd, 1 H, H-1′, $J = 5.9, 8.6$ Hz), 4.61 (d, 1 H, OH-3′, $J = 4.6$ Hz), 4.38 (m, 1H, H-3′), 3.81 [s, 6 H, 2OCH_3-(DMTr)], 3.72 (m, 1 H, CH_2CH_2OTBS), 3.34 (m, 3 H, CH_2CH_2OTBS and H-5′), 2.46 (m, 2 H, H-2′), 2.14 (m, 1 H, CH_2CH_2OTBS), 1.92 (m, 1 H, CH_2CH_2OTBS), 1.42 (s, 3 H, CH_3-5), 0.88 [s, 9 H, Si-C(CH_3)$_3$], 0.07 (s, 3 H, Si-CH_3), 0.02 (s, 3 H, Si-CH_3); HRMS (FAB) calcd for $C_{39}H_{50}N_2NaO_8Si$ 725.3234, found 725.3247 (MNa^+).

3′-Deoxy-5′-O-dimethoxytrityl-4′-C-(2-((tert-butyldimethyl-silyl)oxy)ethyl)thymidine (**9**). A mixture of **8** (0.42 g, 0.60 mmol), 1,1′-thiocarbonyldiimidazole (1.07 g, 6.0 mmol), and pyridine (1.0 mL, 12 mmol) in DMF (6 mL) was stirred at 60 °C for 6 h. The resulting mixture was partitioned between AcOEt and H_2O, and the organic layer was washed with brine, dried (Na_2SO_4), and evaporated. A mixture of the residue, 2,2′-azobis(isobutyronitrile) (AIBN, 198 mg, 1.20 mmol), and Bu_3SnH (1.62 mL, 6.00 mmol) in toluene (12 mL) was heated under reflux for 1 h. The resulting mixture was partitioned between AcOEt and H_2O, and the organic layer was washed with brine, dried (Na_2SO_4), and evaporated. The residue was purified by column chromatography (silica gel; AcOEt/hexane, 1:5−1:2) to give **9** (0.39 g, 95%) as a foam: ^1H NMR ($CDCl_3$, 400 MHz) δ 8.13 (s, 1 H, NH-3), 7.66 (s, 1 H, H-6), 7.13 (m, 13 H, Ar-H), 6.18 (dd, 1 H, H-1′, $J = 6.0, 6.0$ Hz), 3.79 [s, 6 H, 2OCH_3(DMTr)], 3.63 (ddd, 1 H, CH_2CH_2OTBS, $J = 6.0, 6.0, 10.4$ Hz), 3.58 (ddd, 1 H, CH_2CH_2OTBS, $J = 6.0, 6.0, 10.4$ Hz), 3.34 (d, 1 H, H-5′, $J = 10.0$ Hz), 3.18 (d, 1 H, H-5′, $J = 10.0$ Hz), 2.46 (ddd, 1 H, H-2′, $J = 5.0, 8.0, 18.2$ Hz), 2.28 (ddd, 1 H, H-3′, $J = 5.0, 8.0, 14.0$ Hz), 2.13 (ddd, 1 H, H-2′, $J = 8.0, 8.0, 18.2$ Hz), 2.05 (ddd, 1 H, H-3′, $J = 8.0, 8.0, 14.2$ Hz), 1.78 (ddd, 1 H, CH_2CH_2OTBS, $J = 6.0, 6.0, 14.2$ Hz), 1.71 (ddd, 1 H, CH_2CH_2OTBS, $J = 6.0, 6.0, 14.2$ Hz), 1.58 (s, 3 H, CH_3-5), 0.81 [s, 9 H, Si-C(CH_3)$_3$], −0.08 (s, 3 H, Si-CH_3), −0.1 (s, 3 H, Si-CH_3); HRMS (FAB) calcd for $C_{39}H_{50}N_2NaO_7Si$ 709.3285, found 709.3270 (MNa^+).

3′-Deoxy-5′-O-dimethoxytrityl-4′-C-(2-hydroxyethyl)thymidine (**10**). A mixture of **9** (0.42 g, 0.60 mmol) and TBAF (pretreated with molecular sieves 4A, 0.60 g, 2.3 mmol) in THF (6 mL) was stirred at room temperature for 24 h. The resulting mixture was evaporated, and the residue was purified by column chromatography (silica gel; AcOEt/hexane, 10:1) to give **10** (0.32 g, 92%) as a foam: ^1H NMR

($CDCl_3$, 400 MHz) δ 8.08 (s, 1 H, NH-3), 7.52 (s, 1 H, H-6), 7.12 (m, 13 H, Ar-H), 6.21 (dd, 1 H, H-1′, J = 6.8, 6.8 Hz), 3.79 [s, 6 H, 2OCH_3(DMTr)], 3.67 (m, 2 H, CH_2CH_2OH), 3.33 (d, 1 H, H-5′, J = 9.7 Hz), 3.21 (d, 1 H, H-5′, J = 9.7 Hz), 2.45 (m, 1 H, H-2′), 2.32 (m, 1 H, H-3′), 2.13 (m, 1 H, H-2′), 1.98 (m, 2 H, H-3′ and OH), 1.85 (m, 2 H, CH_2CH_2-OH), 1.47 (s, 3 H, CH_3-5); HRMS (FAB) calcd for $C_{33}H_{36}N_2O_7$ 573.2605, found 573.2596 (MH^+).

3′-Deoxy-4′-C-(2-hydroxyethyl)thymidine (**X**). A solution of **10** (143 mg, 0.25 mmol) in aqueous AcOH (80%, 3 mL) was stirred at room temperature for 1 h. The resulting mixture was evaporated, and the residue was purified by column chromatography (silica gel, $CHCl_3$/MeOH, 95:5) to give **X** (22 mg, 33%) as a white solid: ^{1}H NMR (CD_3OD, 400 MHz) δ 7.80 (s, 1 H, H-6), 6.00 (dd, 1 H, H-1′, $J_{1,2\alpha}$ = 4.6 Hz, $J_{1,2\beta}$ = 6.6 Hz, determined by decoupling experiments), 3.58 (m, 3 H, H-5′, CH_2CH_2OH), 3.48 (d, 1 H, H-5′, J = 11.7 Hz), 2.32 (m, 1 H, H-2′β), 2.10 (m, 1 H, H-3′), 1.99 (m, 1 H, H-2′α), 1.83 (m, 4 H, H-3′and CH_3-5), 1.73 (m, 2 H, CH_2CH_2OH); ^{1}H NMR spectrum (400 MHz) was also measured in D_2O, where the $J_{1,2\beta}$ was 4.6 Hz; HRMS (FAB) calcd for $C_{12}H_{19}N_2O_5$ 271.1294, found 271.1303 (MH^+).

Amidite Unit **1**. A mixture of **10** (0.457 g, 0.80 mmol), *N*,*N*-diisopropylethylamine (0.21 mL, 1.2 mmol), and chloro-(2-cyanoethoxy)(*N*,*N*-diisopropylamino)phosphine (0.36 mL, 1.6 mmol) in CH_2Cl_2 (10 mL) was stirred at 0 °C for 30 min. The resulting mixture was partitioned between aqueous saturated $NaHCO_3$ and $CHCl_3$, and the organic layer was washed with brine, dried (Na_2SO_4), and evaporated. The residue was purified by column chromatography (neutral silica gel; AcOEt/hexane, 1:1−1:0) to give **1** (0.35 g, 56%) as a foam: ^{1}H NMR ($CDCl_3$, 270 MHz) δ 7.95 (s, 1 H, NH-3), 7.60 (s, 1 H, H-6), 7.12 (m, 13 H, Ar-H), 6.19 (dd, 1 H, H-1′, J = 10.6 Hz, 6.0 Hz), 3.79 [s, 6 H, 2OCH_3-(DMTr)], 3.62 [m, 6 H, OCH_2CH_2CN and $2NCH(CH_3)_2$], 3.32 (d, 1 H, H-5′, J = 9.9 Hz), 3.19 (d, 1 H, H-5′, J = 9.9 Hz), 2.57 (m, 1 H, H-2′), 2.46 (m, 1 H, H-3′), 2.29 (m, 1 H, H-2′), 2.17 (m, 1 H, H-3′), 1.87 (m, 2 H, CH_2CH_2OP), 1.43 (s, 3 H, CH_3-5), 1.13 [m, 14 H, CH_2CH_2OP and $N(CH(CH_3)_2)_2$]; ^{31}P NMR ($CDCl_3$, 67.5 MHz) δ 148.1, 148.3.

Synthesis of ODNs. ODNs were synthesized on a DNA synthesizer (PE Applied Biosystems, 392 DNA/RNA synthesizer) by the phosphoramidite method. The fully protected ODNs were then deblocked and purified by the same procedure as for the purification of normal ODNs. That is, each ODN linked to the resin was treated with concentrated NH_4OH at 55 °C for 12 h, and the released ODN protected by a DMTr group at the 5′-end was chromatographed on a C-18 silica gel column (1 × 12 cm, Waters) with a linear gradient of MeCN from 5% to 40% in 0.1 M TEAA buffer (pH 7.0). The fractions were concentrated and the residue was treated with aqueous 80% AcOH at room temperature for 20 min; then the solution was evaporated and the residue was coevaporated with H_2O. The residue was dissolved in H_2O and the solution was washed with AcOEt, and then the aqueous layer was evaporated. The residue was purified by HPLC (YMC J's sphere ODS-M80, 150 × 4.6 mm) with a linear gradient of MeCN from 9.5% to 14% in 0.1 M TEAA buffer (pH 7.0) to give a pure ODN. ODN **I-1**: 38.3 OD_{260} units; MS (TOF) calcd for $C_{128}H_{164}N_{48}O_{77}P_{12}$ 3976.7 [$(M - H)^-$], found 3978.7. ODN **I-2**: 36.1 OD_{260} units; MS (TOF) calcd for $C_{140}H_{181}N_{50}O_{84}P_{13}$ 4308.8 [$(M - H)^-$], found 4313.0. ODN **I-3**: 38.4 OD_{260} units; MS (TOF) calcd for $C_{152}H_{198}N_{52}O_{91}P_{14}$ 4640.9 [$(M - H)^-$], found 4641.8. ODN **I-4**: 57.9 OD_{260} units; MS (TOF) calcd for $C_{164}H_{215}N_{54}O_{98}P_{15}$ 4973.0 [$(M - H)^-$], found 4974.4. The yields are indicated in optical density (OD) units at 260 nm starting from 1 μmol scale, and matrix-assisted laser desorption/ionization time-of-flight mass spectra (MALDI-TOF MS) were measured on a Voyager Elite reflection time-of-flight mass spectrometry (PerSeptive Biosystems, Inc.).

Thermal Denaturation. A solution of an ODN (5 or 100 μM) in sodium cacodylate buffer (50 mM, pH 7.0) containing 100 mM of NaCl was heated at 90 °C for 5 min, then cooled gradually to an appropriate temperature, and used for the thermal denaturation studies. Thermal-induced transitions of each mixture were monitored at 260 nm on a Beckman DU 650 spectrophotometer, where sample temperature was increased 0.5 °C/min. Thermodynamic parameters ($\Delta H°$, $\Delta S°$, and $\Delta G°$) for hairpin loop formation were determined by ln K versus T^{-1} plot at 5 μmol concentration of each strand, where K is the equilibrium constant for hairpin loop formation obtained from the UV-melting curve, according to the method reported by Puglisi and Tinoco (*21*).

CD Spectroscopy. CD spectra were measured with a solution of an ODN (15 μM) in sodium cacodylate buffer (50 mM, pH 7.0) containing 100 mM NaCl at 30 °C on a Jasco J720 spectropolarimeter. The ellipticities were recorded from 350 to 200 nm in a cuvette with a path length of 2 mm. CD data were converted into millidegrees per mole of residues per centimeter.

Partial Hydrolysis of ODNs with Nuclease P_1. An ODN labeled with ^{32}P at the 5′-end (20 pmol) in a solution of a Tris-HCl buffer (22 mM, pH 6.8, 90 μL) containing 11 mM $MgCl_2$, 11 μM $ZnAc_2$, and 110 mM KCl was heated at 90 °C for 5 min, and then the mixture was preincubated at 37 °C for 30 min. To the resulting solution was added nuclease P1 (Wako Pure Chemical Co., Ltd., 2.0 units/mL, 5 μL) and the mixture was incubated at 37 °C. At appropriate periods, aliquots (10 μL) of the reaction mixture were separated, which were immediately added to a solution (10 μL) containing EDTA (1 mM), Tris (5 mM), boric acid (5 mM), xylene cyanol FF (0.01%), bromophenol blue (0.05%), and urea (10 M). The solutions were analyzed by electrophoresis on a 20% polyacrylamide gel containing 7 M urea. Densities of radioactivity of the gel were visualized by a bio-imaging analyzer (Bas 2500, Fuji Co., Ltd.).

Molecular Modeling and Calculations. The structures of ODNs **II-1**−**4** were constructed on the basis of the canonical B-form duplex of the ODN 5′-d[CGAACG]-3′ and its complementary ODN 5′-d[CGTTCG]-3′ generated with MOE (version 2003.02, CCG Inc.) and extended with the corresponding length hairpin loop structure ($\mathbf{T_1}$, 1ECU; $\mathbf{T_2}$, 1AC7; $\mathbf{T_3}$, 1OVF; $\mathbf{T_4}$, 1JRN) from the Brookhaven Protein Data Bank. As for ODNs **I-1**−**4**, the phosphodiester linkage of the loop region of each ODN **II** was converted to the 4′-branched-chain region of the nucleoside residue **X**. Molecular mechanics calculations with the OPLS-AA force field were performed in MacroModel (version 8.1, Schrödinger, OR) with the GB/SA continuum solvation model on the eight sequences, ODNs **I-*n*** (n = 1−4) and ODNs **II-*n*** (n = 1−4). The energy minimization was performed by the conjugate gradient method. The resulting three-dimensional structures of ODNs **I-*n*** (n = 1−4) and ODNs **II-*n*** (n = 1−4) were

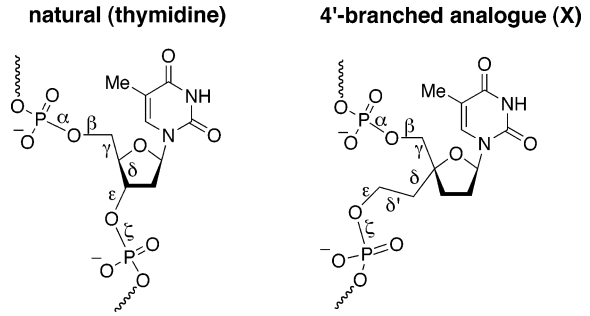

torsion angle	natural	4'-branched analogue (**X**)
α	flexible	flexible
β	restricted	restricted
γ	restricted	restricted
δ	rigid	restricted
δ'		flexible
ε	restricted	flexible
ζ	flexible	flexible

FIGURE 2: Phosphodiester backbones consisting of thymidine and the 4′-branched thymidine analogue **X**.

displayed by MolFeat (version 1.1, FiatLux, Tokyo, Japan) and analyzed with 3DNA (http://rutchem.rutgers.edu/~olson/3DNA) (*22*).

RESULTS AND DISCUSSION

Design of the Nucleoside Component and the Hairpin ODN Sequences. As described above, the nucleobases in the loop moiety are often essential in various biological functions of DNA. To exert these biological functions, the relative distance between the nucleobase and the phosphodiester backbone is important. Therefore, the furanose structure in natural DNA, which effectively restricts the three-dimensional positioning of the nucleobase and the phosphodiester backbone, should be preserved in designing an efficient nucleosidic component of the loop for forming useful hairpin structures. The rigid furanose ring is essential for forming the stable structure of the Watson−Crick base-paired DNA duplex. However, in un-base-paired loop moieties, the furanose ring seems to make the phosphodiester backbone quite constrained, because it significantly restricts the O3′−C3′−C4′−C5′ torsion angle (δ), which is in the range of 130°−150° (*3*). In addition to the rigid δ torsion angle, due to the steric demand of the 3′,5′-phosphodiester backbone passing through the C3′−C4′ bond of a furanose ring, the β, γ, and ϵ torsion angles are considerably conformationally restricted, and accordingly α and ζ are only the two flexible torsion angles in natural DNA backbone (Figure 2). While loops consisting of more than three nucleotidic residues in hairpins seem to be conformationally flexible at least to some extent (*23*, *24*), the shorter loop moieties consisting of two or three residues would be significantly constrained. In fact, conformational analysis of loops of three pyrimidine nucleotides residues has shown that the turned backbone is adjusted only through the flexible α and ζ torsion angles, where most β, γ, and ϵ torsion angles remain unchanged and are located in the regular trans, +gauche, and trans domains (*25*). We speculated that if such conformational restriction of the backbone due to the rigid δ and constrained β, γ, and ϵ torsion angles is relaxed, the hairpin structures would be stabilized. Such release from the conformational restriction was expected to be realized by a branching of the phosphodiester backbone at the 4′-position of the furanose ring. Therefore, we devised a nucleoside analogue having the 4′-branched structure. In addition, the one-carbon-elongated -CH_2-CH_2- chain attached to the 4′-postion could make the backbone even more flexible, which would reduce the strain of the loop backbone, resulting in formation of diverse hairpin loops consisting of various numbers of residues. Replacement of the natural nucleotide loop of the hairpins by significantly conformationally flexible nonnucleotide ethylene glycol linkers resulted in more stable hairpins than the corresponding natural ODN hairpins (*11*), which supports our working hypothesis for use of the flexible 4′-branched nucleoside **X** described here.

On the other hand, the degradation of DNA molecules by nucleases is a serious problem in their use as functional tools or therapeutic agents. It is known that when 4′-branched nucleosides are incorporated into ODNs, the duplexes formed by the ODNs are more resistant to nucleolytic hydrolysis compared with natural ODN duplexes (*20*, *26*). Therefore, from the viewpoint of biological stability, the 4′-branched modification may also have an advantage. In the previous study with four hairpins having a loop consisting of four homolytic natural deoxynucleotide residues, i.e., A_4, G_4, T_4, or C_4, the T_4 loop formed more thermally stable DNA hairpins than the other three homolytic loops (*27*). On the basis of these previous results and considerations, we designed the 4′-branched thymidine analogue **X** as the nucleoside residue for constructing the loop moiety of stable hairpin DNAs. As summarized in Figure 2, the thymidine analogue **X** seems to form a considerably conformationally flexible ODN backbone compared with that of natural thymidine.

Breslauer has revealed that the ODNs 5′-d[CGAACG-N_4-CGTTCG]-3′ (N = A, G, C, T) form stable hairpins possessing a common hexameric stem duplex and an un-base-paired loop of four nucleotides (*27*). The same hexameric stem duplex was also used effectively in a study investigating the suitable length of nonnucleotide linkers as a loop for forming stable hairpins (*11*). Thus, we planned to examine the hairpin stabilizing potency of the 4′-branched thymidine analogue **X** by incorporating it into the loop moiety of the well-established Breslauer sequence forming stable hairpins. We wanted to determine the effect of the number of residues comprising the loop on the hairpin stability. Consequently, one, two, three, and four residue(s) of analogue **X** were planned to be incorporated into the loop moiety. The hexameric stem hairpin structure would be suitable for this study, because it is known to form stable hairpins with a loop consisting of two, three, or four thymidine residues (*28*). Thus, we designed the hairpin-forming ODNs 5′-d[CGAACG-$\mathbf{X}_n$-CGTTCG]-3′ (**I-1**, n = 1; **I-2**, n = 2; **I-3**, n = 3; **I-4**, n = 4), shown in Figure 3, for this study.

Synthesis. The phosphoramidite unit **1**, which was needed for preparing the ODNs containing the designed nucleoside analogue **X**, was synthesized from thymidine (**2**). We previously developed new radical chemistry of a silicon tether using a vinylsilyl group and applied it to the synthesis of the 4′-branched nucleosides (*29*−*32*). The method was also effective in the synthesis of the phosphoramidite unit **1** in this study. As shown in Figure 4, the desired **1** would be

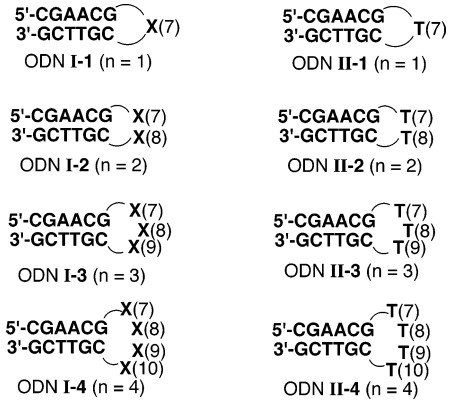

FIGURE 3: Sequences of the modified ODNs **I-1**−**4** and the control natural ODNs **II-1**−**4**.

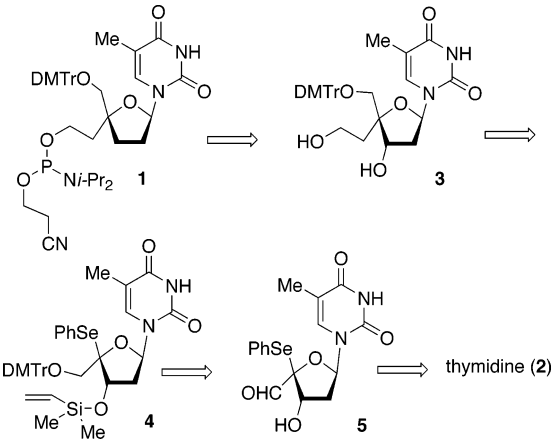

FIGURE 4: Synthetic plan for phosphoramidite unit 1.

derived from the 4′-branched thymidine derivative **3**, which would be obtained with the radical cyclization reaction of **4** as the key step (*20*). The radical reaction substrate **4** could be prepared from thymidine (**2**) via the 4′-phenylselenothymidine derivative **5**.

Synthesis of the phosphoramidite **1** and also the free branched nucleoside **X** is shown in Scheme 1. We have improved the previous procedure for synthesizing **3** (*20*). One-pot treatment of thymidine with TBSCl/imidazole/DMF and then TFA/aqueous THF provided the 3′-*O*-TBS-thymidine (**6**) on a large scale. The previous method for introducing a phenylseleno group at the 4′-position reported by Giese, i.e., the Moffat oxidation of **6** followed by treatment with PhSeCl/Et_3N in CH_2Cl_2 (*19*), was not reproducible, and the yield was significantly lower, especially on large scale. We found that Dess−Martin oxidation (*18*) of **6** followed by treatment with PhSeCl/Et_3N in CH_2Cl_2 was effective for the introduction of a PhSe group at the 4′-position to give **5** in high yield. After conversion of **5** into the branched thymidine derivative **3** according to the previously reported procedure (*20*), the primary hydroxyl of **3** was selectively protected with a TBS group to give **8**. The 3′-deoxygenation of **8** was accomplished via radical reduction of the corresponding 3′-*O*-thiocarbonylimidazolyl intermediate with Bu_3SnH/AIBN. Removal of the silyl protecting group gave the 5′-*O*-dimethoxytritylated 3′-deoxy-4′-branched nucleoside **10**, the subsequent phosphitylation of which by the standard procedure gave the desired phosphoramidite **1**. Deprotection of **10** with aqueous AcOH gave the free nucleoside **X**.

Scheme 1: Synthesis of the Phosphoramidite Unit **1**[a]

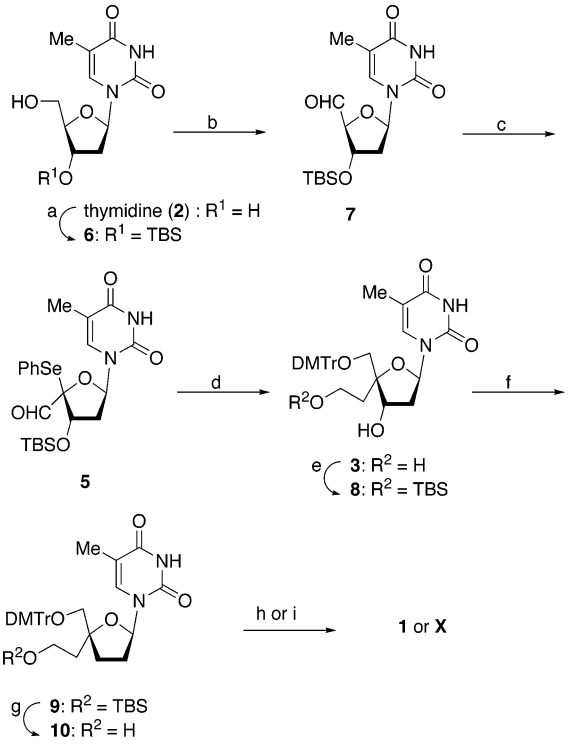

[a] Conditions: (a) (1) TBSCl, imidazole, DMF, rt; (2) TFA, aq THF, 0 °C, 59%. (b) Dess−Martin ox, quant. (c) PhSeCl, Et_3N, CH_2Cl_2, −78 → 0 °C, 83%. (d) Reference 19. (e) TBSOTf, 2,6-lutidine, CH_2Cl_2, −40 °C, 88%. (f) (1) 1,1′-Thiocarbonyldiimidazole, pyridine, DMF, 60 °C; (2) Bu_3SnH, AIBN, toluene, reflux, 95%. (g) Tetrabutylammonium fluoride, THF, 92%. (h) Aqueous AcOH, 33% (**X**). (i) $iPr_2NP(Cl)OCH_2CH_2CN$, iPr_2NEt, CH_2Cl_2, 56% (**1**).

ODNs **I-1**−**4** used in this study were synthesized on a DNA synthesizer by the usual phosphoramidite method. To clarify the property of these ODNs containing the 3′-deoxy-4′-branched nucleoside **X**, the corresponding natural ODNs **II-1**−**4**, i.e., 5′-d[CGAACG-$\mathbf{T}_n$-CGTTCG]-3′ (**II-1**, $n = 1$; **II-2**, $n = 2$; **II-3**, $n = 3$; **II-4**, $n = 4$) containing thymidine (**T**), were also synthesized as controls. The sequences of these ODNs are summarized in Figure 3. Each synthesized ODN showed a single peak on reversed-phase HPLC. Molecular ion peaks supporting their structures were observed in their MALDI-TOF MS.

Thermal Stability. The thermal stability of these hairpin-forming ODNs **I-1**−**4**, as well as the control ODNs **II-1**−**4**, was studied. Thermal denaturation was investigated at 5 μM ODN in a buffer of 50 mM sodium cacodylate (pH 7.0) containing 100 mM NaCl, which showed a single transition corresponding to a helix-to-coil transition. The thermal stability of the ODNs **I-1**−**4** was also measured at 100 μM ODN by the same method. Melting temperatures (T_m) determined from the maximum in the derivative plots of absorbance versus temperature are listed in Table 1. The T_m values of ODNs **I-1**−**4** were all independent of the ODN concentration, which proved that the T_ms were observed depending on their intramolecular structural change, i.e., dissociation of the hairpin structure.

The T_ms of ODNs **I-1**−**4** containing the 4′-branched nucleoside **X** in the loop moiety at 5 μM were 67.1, 68.1, 73.0, and 69.3 °C, respectively, and those of the control natural ODNs **II-1**−**4** were 65.3, 67.0, 69.2, and 68.8, respectively. The thermal stability changed depending on the

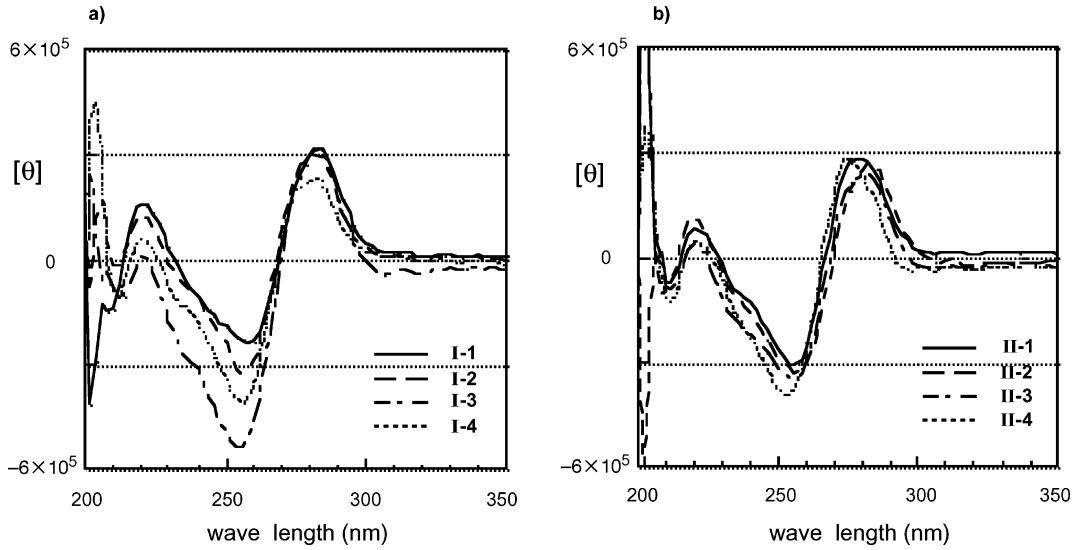

FIGURE 5: CD spectra of the hairpin ODNs **I-1**−**4** (a) and **II-1**−**4** (b).

Table 1: Thermal Melting Temperatures and Thermodynamic Data of ODNs **I-1**−**4** and **II-1**−**4**[a]

ODN (loop)	T_m (°C) at 5 μM[b]	T_m (°C) at 100 μM[b]	$-\Delta H°$ (kcal/mol)	$-\Delta S°$ (eu)	$-\Delta G°_{37}$ (kcal/mol)	ΔT_m[c] (°C) at 5 μM[b]
I-1 (X_1)	67.1	67.2	39.4	115.8	3.5	+1.8
I-2 (X_2)	68.1	68.0	46.7	136.8	4.3	+1.1
I-3 (X_3)	73.0	73.4	52.8	152.7	5.5	+3.8
I-4 (X_4)	69.3	69.4	53.7	156.8	5.1	+0.5
II-1 (T_1)	65.3		34.3	101.8	2.8	
II-2 (T_2)	67.0		43.9	129.0	3.9	
II-3 (T_3)	69.2		47.7	139.1	4.5	
II-4 (T_4)	68.8		46.8	137.2	4.3	

[a] Measured in 50 mM sodium cacodylate buffer (pH 7.0) containing 100 mM NaCl ($n = 3$), and errors in T_m values are within ±1.4%. The thermodynamic parameters were obtained from the UV absorbance melting profiles at 5 μM of ODN, and errors are within ±4.1% for $\Delta H°$, ±4.1% for $\Delta S°$, and ±4.3% for $\Delta G°_{37}$. [b] Concentration of ODN. [c] $\Delta T_m = T_m$(**I-n**) − T_m(**II-n**).

number of the residues (n) comprising the loop, where the order of stability was $n = 3 > n = 4 > n = 2 > n = 1$ in both **I-1**−**4** and **II-1**−**4**. When the number (n) of the loop-forming residues is equal, the T_m of an ODN **I-*n*** is always higher than that of the corresponding ODN **II-*n*** in all cases ($n = 1$−4). The differences in the T_m values (ΔT_m) at 5 μM ODN were 1.8, 1.1, 3.8, and 0.5 °C for $n = 1$−4, respectively. These results clearly show that the 4′-branched nucleoside **X** is able to thermally stabilize the hairpin structures when it is present in the loop moiety. As we speculated, the flexible one-carbon-elongated 4′-branched structure would make this possible.

The thermodynamic parameters were obtained from the UV absorbance melting profiles according to the method reported by Puglisi and Tinoco (*21*). As shown in Table 1, the difference in thermal stability is clearly reflected in the $\Delta G°_{37}$ values. These thermodynamic data suggest that the modified ODNs **I-1**−**4** formed a more stable hairpin than the corresponding unmodified ODNs **II-1**−**4** mainly due to the contribution of $\Delta H°$.

CD Spectra. Circular dichroism (CD) is effective for investigating conformational changes of nucleic acids, and therefore the structures of the ODNs were investigated by CD spectroscopy. CD spectra of the hairpin forming ODNs **I-1**−**4** and the control ODNs **II-1**−**4** at 30 °C are shown in Figure 5.

The CD spectra of ODNs **I-1**−**4** and **II-1**−**4** showed a conservative spectroscopic feature with a positive ellipticity around 280 nm and a negative ellipticity around 250 nm. These spectra are almost identical with those of known stable natural DNA hairpins with a loop consisting of four nucleotide residues, which have a maximum near 280 nm and a minimum near 250 nm (*33*). Furthermore, these spectra are similar to those for typical B-form DNAs (*34*) suggesting that these loops would not severely distort the stem adopting the B-form.

The spectroscopic features of the natural ODNs **II-1**−**4** were similar to each other, while the extent of the negative ellipticity was somewhat different; the rank in strength was **II-4** ($\theta = -4.0 \times 10^5$) > **II-3** ($\theta = -3.5 \times 10^5$) > **II-2** ($\theta = -3.3 \times 10^5$) ≈ **II-1** ($\theta = -3.1 \times 10^5$) (Figure 5 b). On the other hand, the spectra of the ODNs **I-1**−**4** were different from each other (Figure 5a). In particular, the intensity of the negative ellipticity was significantly changed depending on the number of loop residues. The order of intensity is **I-3** ($\theta = -5.4 \times 10^5$) > **I-4** ($\theta = -4.1 \times 10^5$) > **I-2** ($\theta = -3.2 \times 10^5$) > **I-1** ($\theta = -2.4 \times 10^5$), which was same as that for their thermal stability described above. Thus, ODN **I-3**, which had the most thermally stable hairpin structure, showed the deepest negative band. The negative ellipticity may be related to the structural stability of the hairpin ODNs **I-1**−**4**. Since the CD of nucleic acids is mainly dependent on the stacking mode of the bases (*35*), the 4′-branched phosphodiester backbone might change the geometry of the bases in the loop moiety to result in stabilization of the hairpin structure.

Susceptibility to Nuclease P_1. Although hairpins containing a purine loop, such as GAA or GAAA, have been reported to be resistant to nucleases, the hairpins with a pyrimidine-rich loop proved to be hydrolyzed rather easily (*36*). The susceptibility of the ODNs to nucleolytic digestion by the nuclease P_1, an endonuclease, was examined by use of the hairpin-forming ODN **I-3** and **-4**, having an X_3 or an X_4 loop, as well as the corresponding natural ODN **II-3** and **-4**, having a T_3 or a T_4 loop. The ODNs labeled at the 5′-end with ^{32}P were incubated with the enzyme at 37 °C in a

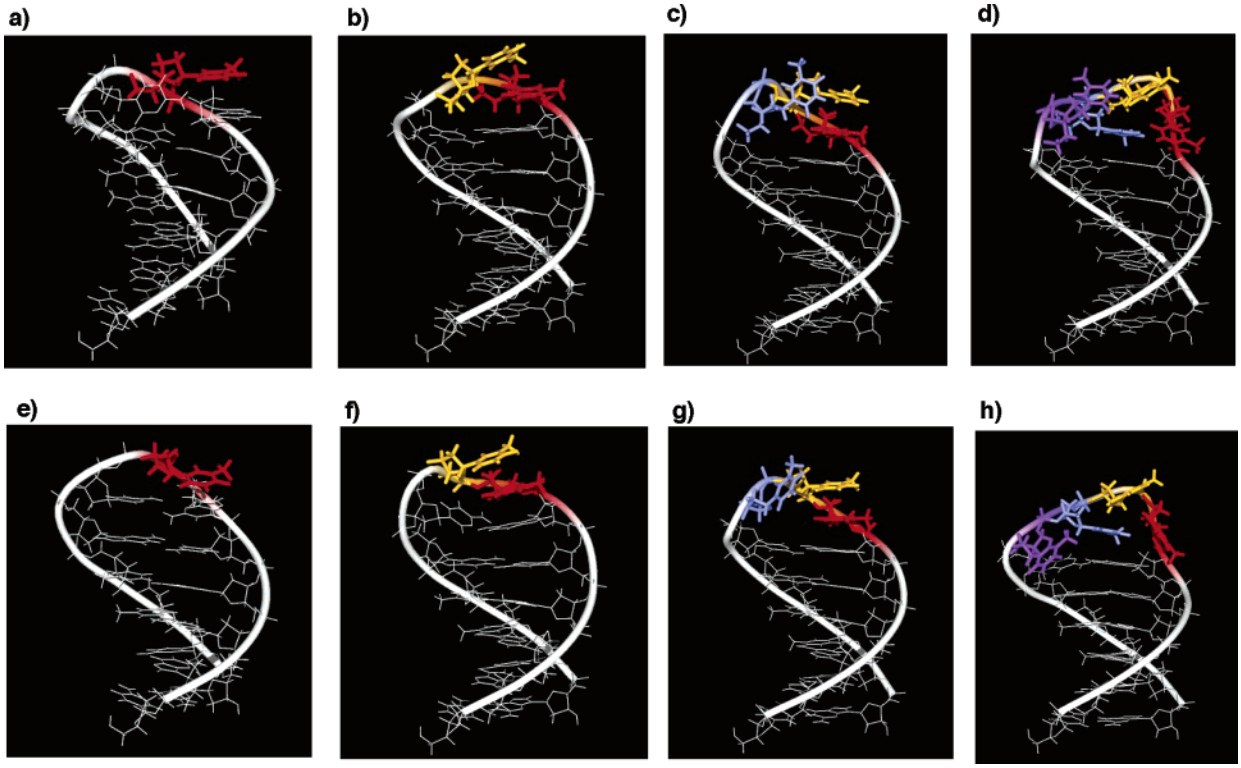

FIGURE 6: Low-energy structures of the hairpin ODNs **I-1** (a), **I-2** (b), **I-3** (c), **I-4** (d), **II-1** (e), **II-2** (f), **II-3** (g), and **II-4** (h) by molecular mechanics calculations: red, **X**(7) and **T**(7); yellow, **X**(8) and **T**(8); light blue, **X**(9) and **T**(9); purple, **X**(10) and **T**(10).

$MgCl_2$-containing buffer (pH 6.8), and the reaction time courses were analyzed by polyacrylamide gel electrophoresis under denaturing conditions. The natural ODN **II-4** was readily hydrolyzed under these conditions and the half-life period ($t_{1/2}$) of decreasing the intact ODN was 11.6 min. However, ODN **I-4** was about twice as resistant to the enzymatic hydrolysis ($t_{1/2}$ = 22.3 min) as ODN **II-4**. ODNs **I-3** and **II-3**, having loops of three residues, were more resistant to the enzyme than ODN **I-4** and **II-4**, having loops of four residues, where the modified ODN **I-3** was more stable than the unmodified ODN **II-3**; after 2 h of incubation under the above conditions, 70% of the intact ODN **I-3** and 46% of the intact **II-3** remained, respectively.

Computational Analysis. We have shown that DNA hairpins containing the sugar-modified thymidine analogue 3′-deoxy-4′-*C*-(2-hydroxyethyl)thymidine (**X**) in the loop moiety (ODN **I**) are more thermally stable than the corresponding natural DNA hairpins (ODN **II**). We further elucidated the mode of the thermal stability of the ODN **I** in comparison to that of the ODN **II** by molecular mechanics calculations to predict their three-dimensional structures.

We employed two construction steps as described below to obtain the appropriate starting structures for the molecular mechanics calculations (*37*−*39*). In the first one, the initial hexameric stem structure was constructed on the basis of a canonical B-form duplex of ODN 3′-d[CGAACG]-5′ and its complementary ODN 3′-d[CGTTCG]-5′ generated with MOE (version 2003.02, CCG Inc., Montreal, Canada), since the CD spectra of all eight ODNs **I-1**−**4** and **II-1**−**4** suggested that the stems adopt a B-form structure. In the second one, the four patterns (**T_1**, **T_2**, **T_3**, and **T_4**) of the hairpin loop on the B-form duplex were used from the data of hairpin loop structures deposited in the Brookhaven Protein Data Bank (n = 1, 1ECU; n = 2, 1AC7; n = 3, 1OVF; n = 4, 1JRN). The low-energy structures of the hairpin loop ODNs obtained by the molecular mechanics calculations are shown in Figure 6.

(1) Hydrogen Bonding and Stacking Interactions of the Thymine Bases in the Loop Moiety. As shown in Figure 6a,e, the calculations for ODNs **I-1** and **II-1** suggested that the G(6)·C(8) loop-closing base pair would not be formed due to the one-residue reverse turning of the backbone. This would be why the one-residue loop ODNs **I-1** and **II-1** were less stable compared with the other hairpin ODNs. However, stacking of the thymine base of **X**(7) (ODN **I-1**) or **T**(7) (ODN **II-1**) to the adjacent G(6) base is observed in both ODNs **I-1** and **II-1**, which can contribute, to some extent, to thermal stability. A hydrogen bond between the 2-O of **X**(7) and the 4-NH_2 of C(8) with a distance of 2.97 Å was observed in ODN **I-1** but not in ODN **II-1**, which might cause a higher T_m for **I-1** than for **II-1** (ΔT_m = 1.8 °C).

In the calculated structures of the ODNs **I-2** and **II-2** having a loop of two residues (Figure 6b,f), the loop thymine base of **X**(7) or **T**(7) stacks with the adjacent G(6) base, while the other thymine base of **X**(8) or **T**(8) protrudes into the solvent and does not participate in any stabilizing interactions. The shape of the G(6)·C(9) loop-closing base pair is different in ODNs **I-2** and **II-2**; the rotation of the base pair of ODN **I-2** is a propeller twist (ω = −12.96), whereas in ODN **II-2** it is a buckle (κ = 48.50). The difference in T_m (ΔT_m = 1.1 °C) between ODNs **I-2** and **II-2** might be due to the more effective G(6)·C(9) base pairing in ODN **I-2** compared with that in ODN **II-2**.

The calculations on the ODNs **I-3** and **II-3** having a loop of three residues supported their stable hairpin structures (Figure 6c,g). In the low-energy structures of both ODNs, the two thymine [**X**(7) and **X**(8) of **I-3** or **T**(7) and **T**(8) of **II-3**] and the G(6) bases are aligned for stable π−π

Table 2: Sugar Puckering of the 4′-Branched Nucleoside (**X**) and Thymidine (**T**) Residues in the Calculated Low-Energy Loop Structures

ODN (loop)	residue	puckering	ODN (loop)	residue	puckering[a]
I-1 (**X**$_1$)	**X**(7)	C2′-endo	**II-1** (**T**$_1$)	**T**(7)	C2′-endo (O4′-endo)
I-2 (**X**$_2$)	**X**(7)	C2′-endo	**II-2** (**T**$_2$)	**T**(7)	C2′-endo (C2′-endo)
	X(8)	C2′-endo		**T**(8)	O4′-endo (C2′-endo)
I-3 (**X**$_3$)	**X**(7)	O4′-endo	**II-3** (**T**$_3$)	**T**(7)	C2′-endo (C2′-endo)
	X(8)	C2′-endo		**T**(8)	C2′-endo (C2′-endo)
	X(9)	C2′-endo		**T**(9)	C2′-endo (C2′-endo)
I-4 (**X**$_4$)	**X**(7)	C3′-endo	**II-4** (**T**$_4$)	**T**(7)	C2′-endo (O4′-endo)
	X(8)	C3′-endo		**T**(8)	C2′-endo (C2′-endo)
	X(9)	C2′-endo		**T**(9)	C2′-endo (C2′-endo)
	X(10)	C2′-endo		**T**(10)	C2′-endo (C2′-endo)

[a] Sugar puckering indicated in parentheses is detected in the crystal structures taken from the Brookhaven Protein Data Bank: **T**$_1$, 1ECU; **T**$_2$, 1AC7; **T**$_3$,1OVF; **T**$_4$, 1JRN.

Table 3: Backbone Torsion Angles[a] of the 4′-Branched Nucleoside (**X**) and Thymidine (**T**) in the Calculated Low-Energy Loop Structures

ODN (loop)	residue	a	b	g	d	d¢	e	z
I-1 (**X**$_1$)	**X**(7)	57.3	−133.1	−42.1	−47.1	−51.8	178.4	65.4
I-2 (**X**$_2$)	**X**(7)	−70.2	173.9	−176.7	−154.7	−64.9	155.9	171.1
	X(8)	−62.1	−159.7	−176.6	178.4	79.2	92.8	−70.2
I-3 (**X**$_3$)	**X**(7)	−72.3	171.9	−176.0	−126.3	−65.4	166.0	−172.6
	X(8)	163.1	178.0	−63.4	−61.9	−71.5	−163.6	77.8
	X(9)	−77.0	119.2	−157.7	−70.8	59.2	168.1	−71.0
I-4 (**X**$_4$)	**X**(7)	−153.7	178.8	−151.0	−60.3	177.5	56.5	−74.5
	X(8)	−56.0	175.3	−168.4	−169.2	75.9	163.6	39.3
	X(9)	−176.2	−177.1	−167.5	−62.1	−74.1	171.8	166.2
	X(10)	−57.4	127.3	−152.5	−65.7	57.2	130.6	−89.4
II-1 (**T**$_1$)	**T**(7)	170.4	177.6	166.1	126.7		−91.4	163.4
II-2 (**T**$_2$)	**T**(7)	178.9	172.2	173.4	135.3		−177.4	−75.0
	T(8)	166.8	−174.7	155.5	98.4		49.3	−66.7
II-3 (**T**$_3$)	**T**(7)	169.8	177.1	168.7	130.7		177.5	−77.3
	T(8)	165.1	179.8	167.1	143.2		−93.1	156.6
	T(9)	69.7	158.6	56.1	145.6		−92.2	53.7
II-4 (**T**$_4$)	**T**(7)	166.4	171.2	163.9	155.0		−88.2	141.9
	T(8)	−74.9	129.3	66.0	137.9		−88.7	169.3
	T(9)	51.3	−153.4	158.9	155.8		−91.2	170.9
	T(10)	49.3	175.5	−70.6	147.7		−77.9	63.7

[a] Torsion angles are given in degrees.

interactions, and the rotation of the G(6)·C(10) loop-closing base pair is very small ($\theta = -0.37$ for **I-3** and 1.68 for **II-3**) indicating their effective hydrogen bonding. These effective interactions would make them relatively stable compared with the other ODNs having a one-, two-, or four-residue(s) loop. Furthermore, an irregular hydrogen bond between the 2-O of **X**(8) and the 3-NH of **X**(9) with distance of 3.05 Å is observed in ODN **I-3**, which could make its T_m higher compared to that of ODN **II-3**.

The calculations on ODNs **I-4** and **II-4** having loops of four residues show that the thymine base of **X**(9) or **T**(9) stacks with the three-residue-distant G(6) base, while the other three thymine bases protrude into the solvent (Figure 6d,h). The rotation of the G(6)·C(11) loop-closing base pair is a buckle in both ODN **I-4** ($\kappa = -12.38$) and ODN **II-4** ($\kappa = -24.53$). The somewhat higher T_m of ODN **I-4** than that of ODN **II-4** might be due to an irregular hydrogen bond between the 2-O of **X**(8) and the 3-NH of **X**(9) with a distance of 3.08 Å observed in ODN **I-4**.

These interactions in the bases of the loop moiety in the calculated low-energy structures are not contradictory to the above experimental results on thermal stability and CD spectral analyses.

(2) Phosphodiester Backbone and Sugar Puckering. The thermal stability of ODNs **I-1**−**4** and control ODNs **II-1**−**4** can be related not only to the interactions between the bases but also to the sugar puckering and phosphodiester backbone conformation in the hairpin loop region.

Sugar puckering of the 4′-branched nucleoside **X** and thymidine residues in the calculated low-energy loop structures of ODNs **I-1**−**4** and control ODNs **II-1**−**4** are summarized in Table 2. The sugar puckering patterns of the thymidine residues in control ODNs **II-1**−**4** are retained in 2′-endo or O4′-endo forms, which are typical in normal DNA duplexes. The thymidine residues in the loop of crystal hairpins are also shown to adopt 2′-endo or O4′-endo forms (**T**$_1$, 1ECU; **T**$_2$, 1AC7; **T**$_3$, 1OVF; **T**$_4$, 1JRN), as shown in the same table. On the other hand, the sugar puckering of **X** in the loop moiety might be more flexible; in the structure of the ODN **I-4**, two of the four 4′-branched residues adopted the C3′-endo form, which is typical in RNA. These data suggest that the 4′-branched phosphodiester linkage could make the sugar puckering flexible compared with that in the usual 3′,5′-phosphodiester linkage.

The flexibility in the sugar puckering in **X** was also shown by its ^{1}H NMR analysis. Namely, in the ^{1}H NMR spectrum of **X** in D_2O, a smaller $J_{1'2'\beta}$ value of 4.6 Hz than that of thymidine ($J_{1'2'\beta} = 6.6$ Hz) was observed, which showed that the population density of the 2′-endo conformer in **X** seems to be not as high as in the natural 2′-deoxynucleosides (*40*).

Backbone torsion angles for the calculated low-energy loop structures of ODNs **I-1**−**4** and control ODNs **II-1**−**4** are summarized in Table 3. The torsion angles of ODNs **I-1**−**4** are largely different from those of ODNs **II-1**−**4**, even when two ODNs having the same number (*n*) of loop residue(s) are compared, e.g., comparison of **I-3** ($n = 3$) and **II-3** ($n = 3$). The difference in the torsion angles between ODN **I-*n*** ($n = 1-4$) and ODN **II-*n*** ($n = 1-4$) would significantly affect their thermal stability. The 4′-branched nucleoside residues can adopt various +gauche, trans, and -gauche torsion angles, especially in the α, *δ*, *δ*′, and *ζ* angles, suggesting that they are actually conformationally flexible in the loop moiety to form stable hairpins.

This conformational flexibility of the 4′-branched nucleoside **X** in the sugar puckering and also in the phosphodiester backbone of the loop moiety may contribute to the stabilization of hairpin structures by the effective formation of the hydrogen bonds described above. This is supported by the thermodynamic data suggesting that the thermal stabilization by the loops of the branched 4′-branched nucleoside **X** is mainly due to the advantage for $\Delta H°$, as shown in Table 1.

CONCLUSION

The sugar-modified thymidine analogue 3′-deoxy-4′-*C*-(2-hydroxyethyl)thymidine (**X**), designed as a loop component for stabilizing hairpin structures, was synthesized from thymidine. Experimental studies and calculations on the hexameric stem of the hairpin ODNs containing $\mathbf{X}_n$ ($n = 1-4$) in the loop moiety showed that **X** was able to stabilize the hairpin structures. The hairpin-stabilizing property of **X** would be due to the flexible one-carbon-elongated 4′-branched structure. Thus, the unit **X** may be applicable to the development of functional DNA molecules having hairpin loops.

ACKNOWLEDGMENT

We are grateful to Professor Naoki Sugimoto (Konan University) for his helpful suggestion on the measurement of thermal stability of ODNs and to Ms. H. Matsumoto, A. Maeda, and S. Oka (Center for Instrumental Analysis, Hokkaido University) for technical assistance with NMR, MS, and elemental analyses.

REFERENCES

1. Varani, G. (1995) Exceptionally stable nucleic acid hairpins, *Annu. Rev. Biophys. Biomol. Struct. 24*, 379−404.
2. Glucksmann-Kuis, M. A., Dai, X., Markiewicz, P., and Rothaman-Denes, L. B. (1996) *E. coli* SSB activates N4 virion RNA polymerase promoters by stabilizing a DNA hairpin required for promoter recognition, *Cell 84*, 147−154.
3. Zacharias, M. (2001) Conformational analysis of DNA-trinucleotide-hairpin-loop structures using a continuum solvent model, *Biophys. J. 80*, 2350−2363.
4. Sun, L. Q., Cairns, M. J., Saravolac, E. G., Baker, A., and Gerlach, W. L. (2000) Catalytic nucleic acids: from lab to applications, *Pharmacol. Rev. 52*, 325−347.
5. Li, Y., and Breaker, R. R. (1999) Deoxyribozymes: new players in the ancient game of biocatalysis, *Curr. Opin. Struct. Biol. 9*, 315−323.
6. Hirao, I., Yoshizawa, S., and Miura, K. (1993) Stabilization of mRNA in an *Escherichia coli* cell-free translation system, *FEBS Lett. 321*, 169−172.
7. Tang, J. Y., Temsamani, J., and Agrawal, S. (1993) Self-stabilized antisense oligodeoxynucleotide phosphorothioates: properties and anti-HIV activity, *Nucleic Acids Res. 21*, 2729−2735.
8. Khan, I. M., and Coulson, J. M. (1993) A novel method to stabilise antisense oligonucleotides against exonuclease degradation, *Nucleic Acids Res. 21*, 2957−2958.
9. Hosoya, T., Takeuchi, H., Kanesaka, Y., Yamakawa, H., Miyano-Kurosaki, N., Takai, K., Yamamoto, N., and Takaku, H. (1999) Sequence-specific inhibition of a transcription factor by circular dumbbell DNA oligonucleotides, *FEBS Lett. 461*, 136−141.
10. Demidov, V. V. (2001) DNA dumbbells: decoys for gene-regulatory proteins, *Drug Discovery Today 6*, 749−750.
11. Rumney, S., IV, and Kool, E. T. (1995) Structural optimization of nonnucleotide loop replacements for duplex and triplex DNAs, *J. Am. Chem. Soc. 117*, 5635−5646.
12. Lewis, F. D., Wu, Y., and Liu, X. (2002) Synthesis, structure, and photochemistry of exceptionally stable synthetic DNA hairpins with stilbene diether linkers, *J. Am. Chem. Soc. 124*, 12165−12173.
13. Yoshizawa, S., Dawai, G., Watanabe, K., Miura, K., and Hirao, I. (1997) Abstract GNA trinucleotide loop sequences producing extraordinarily stable DNA minihairpins, *Biochemistry 36*, 4761−4767.
14. Chou, S.-H., Tsung, Y.-Y., and Wang, S.-W. (1999) Stable sheared A-*C* pair in DNA hairpins, *J. Mol. Biol. 287*, 301−313.
15. Amri, C. E., Mauffret, O., Monnot, M., Tevanian, G., Lescot, E., Porumb, H., and Fermandjian, S. (1999) A DNA hairpin with a single residue loop closed by a strongly distorted Watson−Crick G-*C* base-pair, *J. Mol. Biol. 294*, 427−442.
16. Katz, R. A., Gravuer, K., and Skalka, A. M. (1998) A preferred target DNA structure for retroviral integrase in vitro, *J. Biol. Chem. 273*, 24190−24195.
17. Connelly, J. C., Kirkham, L. A., and Leach, D. R. (1998) The SbcCD nuclease of *Escherichia coli* is a structural maintenance of chromosomes (SMC) family protein that cleaves hairpin DNA, *Proc. Natl Acad. Sci. U.S.A. 95*, 7969−7974.
18. Dess, D. B., and Martin, J. C. (1991) A useful 12-I-5 triacetoxyperiodinane (the Dess−Martin periodinane) for the selective oxidation of primary or secondary alcohols and a variety of related 12-I-5 species, *J. Am. Chem. Soc. 113*, 7277−7287.
19. Giese, B., Erdmann, P., Schafer, T., and Schwitter, U. (1994) Synthesis of a 4α-selenated 2-deoxyadenosine derivative: a novel precursor suitable for the preparation of modified oligonucleotides, *Synthesis* 1310−3112.
20. Ueno, Y., Nagasawa, Y., Sugimoto, I., Kojima, N., Kanazaki, M., Shuto, S., and Matsuda, A. (1998) Synthesis of oligodeoxynucleotides containing 4′-*C*-[2-[*N*-(2-aminoethyl)carbamoyl]oxy]thymidine and their thermal stability and nuclease-resistance ptoperties, *J. Org. Chem. 63*, 1660−1667.
21. Puglisi, J. D., and Tinoco, I. (1989) Absorbance melting curves of RNA, *Methods Enzymol. 180*, 304−325.
22. Lu, X. J., and Olson, W. K. (2003) 3DNA: a software package for the analysis, rebuilding and visualization of three-dimensional nucleic acid structures, *Nucleic Acids Res. 31*, 5108−5121.
23. Chatopadhyaya, R., Ikuta, S., Grezeskowiak, K., and Dickerson, R. E. (1988) X-ray structure of a DNA hairpin molecule, *Nature 334*, 175−179.
24. Hare, D. R., and Reid, B. R. (1986) Three-dimensional structure of a DNA hairpin in solution: two-dimensional NMR studies and distance geometry calculations on d(CGCGTTTTCGCG), *Biochemistry 25*, 5341−5350.
25. Chou, S.-H., Tseng, T.-Y., and Chu, B.-Y. (1999) Stable formation of a pyrimidine-rich loop hairpin in a cruciform promoter, *J. Mol. Biol. 292*, 309−320.
26. Kanazaki, M., Ueno, Y., Shuto, S., and Matsuda, A. (2000) Highly nuclease-resistant phosphodiester-type oligodeoxynucleotides containing 4′α-*C*-aminoalkylthymidines form thermally stable duplexes with DNA and RNA. A candidate for potent antisense molecules, *J. Am. Chem. Soc. 122*, 2422−2432.
27. Senior, M. M., Jones, R. A., and Breslauer, K. J. (1988) Influence of loop residues on relative stabilities of DNA hairpin structures, *Proc. Natl. Acad. Sci. U.S.A. 85*, 6242−6246.
28. Xodo, L. E., Manzini, G., Quadrifoglio, F., van der Marel, G., and van Boom, J. (1991) DNA hairpin loops in solution. Correlation between primary structure, thermostability and reactivity with single-strand-specific nuclease from mung bean, *Nucleic Acid Res. 19*, 1505−1511.
29. Shuto, S., Kanazaki, M., Ichikawa, S., and Matsuda, A. (1997) A novel ring-enlargement reaction of (3-oxa-2-silacyclopentyl)methyl radicals into 4-oxa-3-silacyclohexyl radicals. Stereoselective introduction of a hydroxyethyl group via unusual 6-*endo*-cyclization products derived from 3-oxa-4-silahexenyl radicals, and its

application to the synthesis of a 4′α-branched nucleoside, *J. Org. Chem. 62*, 5676−5677.
30. Shuto, S., Kanazaki, M., Ichikawa, S., Minakawa, N., and Matsuda, A. (1998) Stereo- and regioselective introduction of 1- or 2-hydroxyethyl group via intramolecular radical cyclization reaction with a novel silicon-containing tether. An efficient synthesis of 4′α-branched 2′-deoxyadenosines, *J. Org. Chem. 63*, 746−754.
31. Sugimoto, I., Shuto, S., and Matsuda, A. (1999) A one-pot method for the stereoselective introduction of a vinyl group via an atom transfer radical cyclization reaction with a diphenylvinylsilyl group as a temporary connecting tether. Synthesis of 4′α-*C*-vinylthymidine, a potent antiviral nucleoside, *J. Org. Chem. 64*, 7153−7157.
32. Shuto, S., Sugimoto, I., and Matsuda, A. (2000) Mechanistic study of the ring-enlargement reaction of (3-oxa-2-silacyclopentyl)-methyl radicals into 4-oxa-3-silacyclohexyl radicals. Evidence for a pentavalent silicon-bridging radical transition state in 1,2-rearrangement reactions of *β*-silyl radicals, *J. Am. Chem. Soc. 122*, 1343−1351.
33. Nakano, M., Moody, E. M., Liang, J., and Bevilacqua, P. C. (2002) Selection for thermodynamically stable DNA tetraloops using temperature gradient gel electrophoresis reveals four motifs: d(cGNNAg), d(cGNABg), d(cCNNGg), and d(gCNNGc), *Biochemistry 41*, 14281−14292.
34. Tunis-Schneider, M. J., and Maestre, M. F. (1970) Circular dichroism spectra of oriented and unoriented deoxyribonucleic acid films—a preliminary study, *J. Mol. Biol. 52*, 521−541.
35. Bloomfield, V. A., Crothers, D. M., and Tinoco, I., Jr. *Nucleic Acids—Structure, Properties, and Functions*, pp 185−198, University Science Books, Sausalito, CA, 2000.
36. Yoshizawa, S., Ueda, T., Ishido, Y., Miura, K., Watanabe, K., and Hirao, I. (1994) Nuclease resistance of an extraordinarily thermostable mini-hairpin DNA fragment, d(GCGAAGC) and its application to in vitro protein synthesis, *Nucleic Acids Res. 22*, 2217−2221.
37. Ide, H., Shimizu, H., Kimura, Y., Sakamoto, S., Makino, K., Glackin, M., Wallace, S. S., Nakamuta, H., Sasaki, M., and Sugimoto, N. (1995) Influence of alpha-Deoxyadenosine on the Stability and Structure of DNA. Thermodynamic and Molecular Mechanics Studies, *Biochemistry 34*, 6947−6955.
38. Lind, K. E., Mohan, V., Manoharan, M., and Ferguson, D. M. (1998) Structural characteristics of 2′-O-(2-methoxyethyl)-modified nucleic acids from molecular dynamics simulations, *Nucleic Acids Res. 26*, 3694−3799.
39. Christensen, U. B., and Pedersen, E. B. (2002) Intercalating nucleic acids containing insertions of 1-O-(1-pyrenylmethyl)glycerol: stabilisation of dsDNA and discrimination of DNA over RNA, *Nucleic Acids Res. 30*, 4918−4925.
40. Seio, K., Wada, T., Sakamoto, K., Yokoyama, S., and Sekine, M. (1996) Chemical synthesis and conformational properties of a new cyclouridylic acid having an ethylene bridge between the uracil 5-position and 5′-phosphate group, *J. Org. Chem. 61*, 1500−1504.

BI0496283